Check for updates

Geophysical Research Letters

RESEARCH LETTER
10.1029/2023GL105332

Two Competing Drivers of the Recent Walker Circulation Trend

Masahiro Watanabe[1], Tomoki Iwakiri[2], Yue Dong[3], and Sarah M. Kang[4]

[1]Atmosphere and Ocean Research Institute, University of Tokyo, Kashiwa, Japan, [2]Meteorological Research Institute, Tsukuba, Japan, [3]Lamont-Doherty Earth Observatory, Columbia University, Palisades, NY, USA, [4]Max Planck Institute for Meteorology, Hamburg, Germany

Key Points:

- The past strengthening trend of the Pacific Walker circulation (PWC) is well reproduced in the AMIP simulations
- PWC weakens with surface warming consistent with global energy constraints, but the effect cannot overcome the pattern effect on circulation
- The pattern effect originates directly from the SST trend in the equatorial band, to which Indian Ocean warming contributes by about 30%

Supporting Information:

Supporting Information may be found in the online version of this article.

Correspondence to:

M. Watanabe,
hiro@aori.u-tokyo.ac.jp

Citation:

Watanabe, M., Iwakiri, T., Dong, Y., & Kang, S. M. (2023). Two competing drivers of the recent Walker circulation trend. *Geophysical Research Letters*, *50*, e2023GL105332. https://doi.org/10.1029/2023GL105332

Received 18 JUL 2023
Accepted 30 AUG 2023

Author Contributions:

Conceptualization: Masahiro Watanabe, Sarah M. Kang
Formal analysis: Masahiro Watanabe, Tomoki Iwakiri, Yue Dong
Investigation: Masahiro Watanabe
Methodology: Masahiro Watanabe, Yue Dong, Sarah M. Kang
Validation: Masahiro Watanabe, Tomoki Iwakiri
Visualization: Masahiro Watanabe, Tomoki Iwakiri, Yue Dong
Writing – original draft: Masahiro Watanabe
Writing – review & editing: Yue Dong, Sarah M. Kang

© 2023 The Authors.
This is an open access article under the terms of the Creative Commons Attribution-NonCommercial License, which permits use, distribution and reproduction in any medium, provided the original work is properly cited and is not used for commercial purposes.

Abstract The Pacific Walker circulation (PWC) weakens under global warming in climate change projections, supported by a global hydrological constraint. However, the PWC has strengthened over the past decades despite ongoing global warming, and the cause has been a puzzle. Because PWC is coupled with the pattern of sea surface temperature (SST) in the tropical Pacific, quantifying the relative impact of SST pattern change and global warming on the past PWC trend is important. We show, using an atmosphere model driven by observed boundary conditions for 1979–2013 and a hypothetical uniform surface warming trend with varying magnitude, that the PWC scales with warming and weakens by 8% per °C, but this effect cannot overcome the SST pattern effect that intensifies the circulation. Further attribution experiments show that the past strengthening of PWC is explained directly by the SST warming pattern in the narrow equatorial band, about 30% of which is induced by the Indian Ocean.

Plain Language Summary The large-scale overturning circulation in the tropical Pacific known as the Pacific Walker circulation is the heart of the general circulation of the atmosphere. Most of the future climate projections by climate models suggest that the Walker circulation weakens with surface warming. However, observations show that the circulation has strengthened over the past decades despite ongoing global warming. We show, using atmosphere model simulations for 1979–2013 that the Walker circulation strengthening is well reproduced and it weakens when a hypothetical uniform surface warming trend was imposed on the sea surface temperature (SST) data that force the model. The weakening of the Walker circulation occurs at a rate of about 8% per degree warming, but this effect cannot overcome the SST pattern effect that intensifies the circulation. Further attribution simulations show that the past strengthening is explained directly by the SST warming pattern in the narrow equatorial band, about one-third of which is induced by the warming of the Indian Ocean.

1. Introduction

The atmosphere and ocean are strongly tied in the tropical Pacific, forming the Pacific Walker circulation (PWC) and a set of warm pool/cold tongue. They maintain each other in a way that the zonal gradient in sea surface temperature (SST) drives the easterly trades, a surface manifestation of PWC, and the trade winds in turn pile warm water up to the western Pacific as well as cool the eastern Pacific via ocean upwelling. This process, called the Bjerknes feedback (Bjerknes, 1969), explains not only mean states and El Niño-Southern Oscillation (ENSO) (Jin, 1996) but also a part of climate change patterns in response to greenhouse gas (GHG) increase (Xie, 2022). In the instrumental measurement period since the late 19th century, recent decades are marked by a particularly large intensification trend of the PWC and the zonal SST gradient (England et al., 2014) and the cause has long been controversial. The magnitude and sign of the trend depend on the period but it was the largest positive over the recent decades (Figure S1 in Supporting Information S1), so we take a 35 years period of 1979–2013 when calculating the trends in this study.

The global pattern of SST trends for 1979–2013 is characterized by warming except in the eastern Pacific and the Southern Ocean (Figure S1 in Supporting Information S1). Consistent with the enhanced zonal SST gradient in the equatorial Pacific, sea-level pressure (SLP) trends are negative in the west and positive in the east, indicating that the PWC is also intensified. Their metrics, the zonal SST gradient in the equatorial Pacific defined as the SST difference between the central-eastern Pacific (180°–80°W, 5°S–5°N) and the western Pacific (80°–150°E, 5°S–5°N) (Heede & Fedorov, 2021) and the Walker circulation index defined as a SLP difference

between the central-eastern Pacific (160°−80°W, 5°S–5°N) and warm pool region (80°−160°E, 5°S–5°N) (Vecchi et al., 2006), are significantly correlated at the interannual time scale, and the 35 years trends lie in the linear relationship (Figure S1d in Supporting Information S1). Because the pattern of SST trends is similar to the well-known Interdecadal Pacific Oscillation (IPO), an internal mode of variability in the Pacific (Henley et al., 2017; Power et al., 1999), the recent trends in the SST gradient and the PWC are often considered to arise from the negative IPO (Bordbar et al., 2017; Coats & Karnauskas, 2017; Lee et al., 2022).

The active role of such natural variability in the observed multi-decadal trend has been supported by analyses of large ensembles of global climate model (GCM) simulations (Chung et al., 2019; Watanabe et al., 2021; Wu et al., 2021). However, it is becoming clear that the climate model simulations are systematically biased to generate a weakening of the zonal contrast in SST and SLP over the past decades (Wills et al., 2022), leading to suspicion that the models do not adequately represent a forced response to GHGs or aerosols due perhaps to errors in the coupled mean state in the Pacific (Seager et al., 2019, 2022). There are several mechanisms to explain the observed strengthening, for example, aerosol forcing (Smith et al., 2016; Takahashi & Watanabe, 2016), remote effect of the Southern Ocean cooling (Dong et al., 2022; England et al., 2020; Kang et al., 2023; Kim et al., 2022), and coupling with tropical Atlantic and Indian Oceans (Li et al., 2016; McGregor et al., 2014; O'Reilly et al., 2023), but they are based on the potentially biased coupled model simulations, hindering a robust attribution of the past PWC intensification.

2. Attribution of the Observed PWC Intensification

2.1. Advantage of Using Atmosphere-Only Simulations for the Attribution

Climate simulations using an atmospheric component of GCM, driven by the observed history of SST, sea ice, and radiative forcing such as GHGs and aerosols, are called the Atmospheric Model Intercomparison Project (AMIP) experiment (Gates et al., 1999), which is part of the Coupled Model Intercomparison Project Phase 6 (CMIP6) archive (Eyring et al., 2016). Because the AMIP simulation is free from systematic bias in the mean SST, it reproduces the past variability and change in some aspects of climate such as precipitation and radiative budgets (Loeb et al., 2020; Zhou et al., 2018). It is also true that the PWC trend for 1979–2013 in terms of the pattern and the magnitude is well reproduced by an ensemble of AMIP simulations (Figure 1). Because the tropical atmosphere tends to obey the underlying SST and is less affected by stochastic weather disturbances than the extratropics, the ensemble spread is very small and the results are even quite similar across different models (Figure S2 and Text S1 in Supporting Information S1). This indicates that we can make a robust attribution of the PWC trend using the AMIP simulation but with trading off a weakness: we cannot explore mechanisms for the PWC intensification mediated by atmosphere-ocean coupled processes, which are beyond the scope of this study.

2.2. Hydrological Constraint

A discrepancy in the past PWC trend between observations and coupled models may affect the reliability of future projections. The weakening of PWC simulated in the historical simulations is continuous and amplified in future scenario simulations (Heede & Fedorov, 2021; IPCC, 2021). The most likely process that weakens the PWC has been provided by a global hydrological constraint (Held & Soden, 2006, hereafter referred to as the HS mechanism; see Text S2 in Supporting Information S1). Namely, tropical vertical mass flux, M, has to decrease in a warmed climate given that precipitation increase (ΔP) cannot exceed water vapor increase (Δq), the former controlled by the atmospheric energy balance whereas the latter determined by the Clausius–Clapeyron (CC) relationship. The mass flux reduction has been identified in global warming simulations by GCMs with various configurations and is a solid feature of climate change (Chadwick et al., 2013; He & Soden, 2015; Vecchi & Soden, 2007).

The HS mechanism has also been employed vaguely to explain the centennial-scale weakening of tropical circulation in the 20th century (Tokinaga et al., 2012; Vecchi et al., 2006). However, quantitative assessments claim that the HS mechanism does not work for the PWC trend over the past decades (Heede et al., 2020; Merlis & Schneider, 2011; Sandeep et al., 2014). Indeed, the proponents of the mechanism acknowledge that *a reduction in the mass exchange in the tropics does not necessarily entail a proportional reduction in the strength of the mean tropical circulation* (Held & Soden, 2006). Therefore, it is still an open question to ask why the HS mechanism cannot be identified in the present climate which already experiences global warming of about 1°C. We show in

19448007, 2023, 23, Downloaded from https://agupubs.onlinelibrary.wiley.com/doi/10.1029/2023GL105332 by Cochrane Germany, Wiley Online Library on [12/12/2023]. See the Terms and Conditions (https://onlinelibrary.wiley.com/terms-and-conditions) on Wiley Online Library for rules of use; OA articles are governed by the applicable Creative Commons License

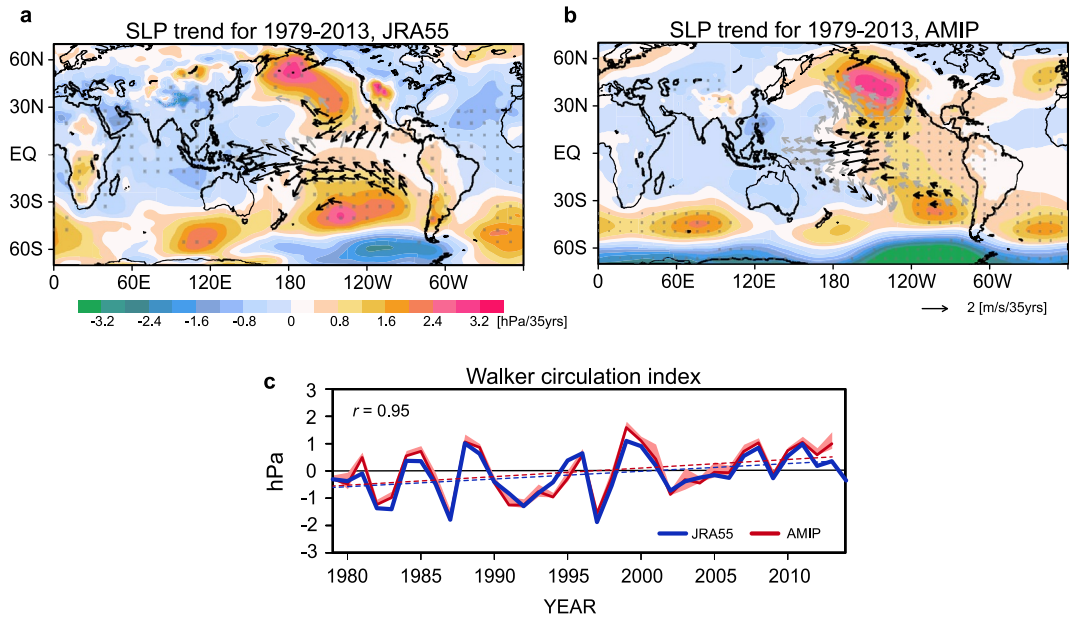

Figure 1. Walker circulation intensification for 1971–2013. (a, b) Linear trends in SLP (shading) and surface winds (vector) for the Japanese 55-Year Reanalysis (JRA55) data (Kobayashi et al., 2015) and the ensemble mean of the MIROC6 AMIP experiment. The stippling denotes that the SLP trends are statistically significant at the 95% level. The wind trends are plotted over the Pacific, with those significant at the 95% level in black and the 90% level in gray. (c) Time series of the Walker index in JRA55 (blue) and the AMIP (red), with the linear trends by dashed lines. The positive value indicates strengthening in the Pacific Walker circulation. The ensemble range (maximum and minimum) is shown by shading. The correlation coefficient between the time series is indicated in the panel.

this study that the PWC actually weakens scaled with surface warming consistent with the prediction by the HS mechanism, but the effect of the past SST pattern change overcomes and acts to intensify the PWC. It has been recognized that the evolving surface warming pattern modulates climate feedbacks—called the pattern effect (IPCC, 2021; Stevens et al., 2016). The pattern effect on the PWC has a different meaning but is closely related to the effect on the feedbacks because the latter happens via changing the tropical circulation (Andrews et al., 2018; Ceppi & Gregory, 2017; Dong et al., 2019; Zhou et al., 2016).

2.3. AMIP-Trend Experiment

For understanding future changes in the tropical circulation and precipitation patterns, AMIP-type experiments with either uniform or patterned warming in SST have been used (Chadwick et al., 2014; He & Soden, 2015; Huang et al., 2013; Xie et al., 2010). Such simulations, including a conventional experiment with a uniform SST increase by 4 K (AMIP+4K), are irrelevant to isolate the effect of evolving global warming on the PWC trend reproduced in the AMIP run.

Therefore, we conducted a series of AMIP runs driven by observed SST on which a hypothetical global-mean SST trend was imposed, called the AMIP-trend experiment. The experiment was carried out using the atmospheric component model of MIROC6 (Tatebe et al., 2019), which has a horizontal resolution of 1.4° in longitude and latitude and 81 vertical layers. The boundary conditions to drive the model are the same as those for the CMIP6 AMIP experiment except the SST data replaced with the National Oceanic and Atmospheric Administration Extended Reconstructed SST version 5 (ERSSTv5) (Huang et al., 2017). There are several SST data sets containing observational uncertainty, but their difference in the tropical Pacific SST trends after around 1950 is small (Watanabe et al., 2021), and indeed the CMIP6 AMIP simulations driven by the AMIP-SST data show a very similar trend to our AMIP run forced by ERSSTv5 (Figure 1c and Figure S2 in Supporting Information S1).

In addition to the conventional AMIP run which is regarded as a reference, we performed four experiments by re-scaling the global-mean SST anomaly time series to have the linear trend of 0, 1, 2, and 4K for 1979–2013, with other boundary conditions unchanged (Figure S3 in Supporting Information S1). The globally uniform SST

19448007, 2023, 23, Downloaded from https://agupubs.onlinelibrary.wiley.com/doi/10.1029/2023GL105332 by Cochrane Germany, Wiley Online Library on [12/12/2023]. See the Terms and Conditions (https://onlinelibrary.wiley.com/terms-and-conditions) on Wiley Online Library for rules of use; OA articles are governed by the applicable Creative Commons License

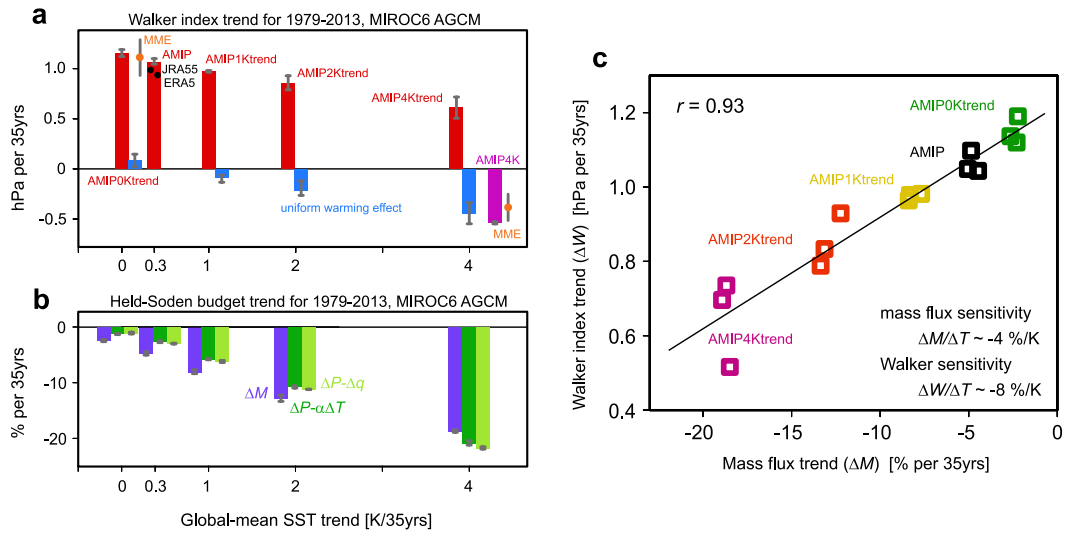

Figure 2. Attribution of the Pacific Walker circulation trend to the SST pattern and uniform warming. (a) Linear trend of the Walker index in the AMIP-trend experiments (red) and the difference from the trend in AMIP (blue). The trend in AMIP+4K (purple) is shown for comparison. The error bar represents the maximum-minimum range. The orange dot with the gray line indicates the mean and the standard deviation of the trends from the CMIP6 multi models. (b) As in (a) but for the trend in the global hydrological budgets from the AMIP-trend experiments: ΔM (blue), ΔP-Δq (light green), and ΔP-$\alpha\Delta T$ (green), all presented as a fractional change against their climatological mean. We used precipitable water as q whereas the convective mass flux derived from parameterization schemes and integrated for 925–700 hPa as M. (c) Scatter plot between the 35 years trends in the mass flux (ΔM) and the Walker index (ΔW), respectively. Their correlation coefficient, regression line, and sensitivity to warming are shown in the panel.

perturbation was applied for each month without changing the pattern of local SST trends. These experiments are referred to as AMIP+0Ktrend, AMIP+1Ktrend, AMIP+2Ktrend, and AMIP+4Ktrend experiments. It is noted that there is no global-mean SST trend in AMIP+0Ktrend over the whole period. Each experiment has three members and all simulations span from 1978 to 2015.

3. Role of Uniform Warming and the Pattern Change in the PWC Intensification

Figure 2a shows the linear trends in the Walker index for 1979–2013 obtained from the MIROC6 AMIP-trend experiments. It is evident that the PWC does weaken in proportion to global warming, and at the same time, the effect of uniform warming is not enough to change the sign of the PWC trend even with the +4K warming trend, which only accounts for about half of the PWC trend in AMIP. It is thus reasonable that the uniform warming impact on the PWC trend can hardly be detected at the present global warming level (0.29 K in global-mean SST over the period) as found in little difference between the AMIP and AMIP+0Ktrend. The relative slowdown of the PWC in AMIP+4Ktrend is slightly weaker than that in AMIP+4K but the difference is within the uncertainty range.

The weakening of the PWC trend with uniform warming in the AMIP-trend experiments is consistent with the HS mechanism (Figure 2b). Changes in the global hydrological budgets are roughly balanced between the convective mass flux change (ΔM) and the atmospheric water amount change (ΔP-Δq), the latter further approximated using the CC relationship as ΔP-$\alpha\Delta T$, where $\alpha = 7\%\ \mathrm{K}^{-1}$. In this study, we used the convective mass flux derived from parameterization schemes as M and then integrated it over 925–700 hPa. The reduction of the mass flux and the PWC weakening are highly correlated across the ensemble (five experiments and three members for each), showing the correlation coefficient of $r = 0.93$ (Figure 2c). The sensitivity of mass flux reduction to warming, about $4\%\ \mathrm{K}^{-1}$, is consistent with the global precipitation increase of 2%–$3\%\ \mathrm{K}^{-1}$ (DeAngelis et al., 2015; Fläschner et al., 2016), whereas the PWC weakens more sensitively to surface warming with about 8% per °C, although the reason of higher sensitivity is not very clear. However, this weakening tendency cannot overcome the strengthening due to the SST pattern effect as represented by the y-intercept showing a large PWC strengthening without reduction in M (Figure 2c). The result in Figure 2 also shows that the reduction in the mass flux and the strengthening of the PWC can coexist in the AMIP simulation, consistent with a recent study (Shrestha & Soden, 2023).

19448007, 2023, 23, Downloaded from https://agupubs.onlinelibrary.wiley.com/doi/10.1029/2023GL105332 by Cochrane Germany, Wiley Online Library on [12/12/2023]. See the Terms and Conditions (https://onlinelibrary.wiley.com/terms-and-conditions) on Wiley Online Library for rules of use; OA articles are governed by the applicable Creative Commons License

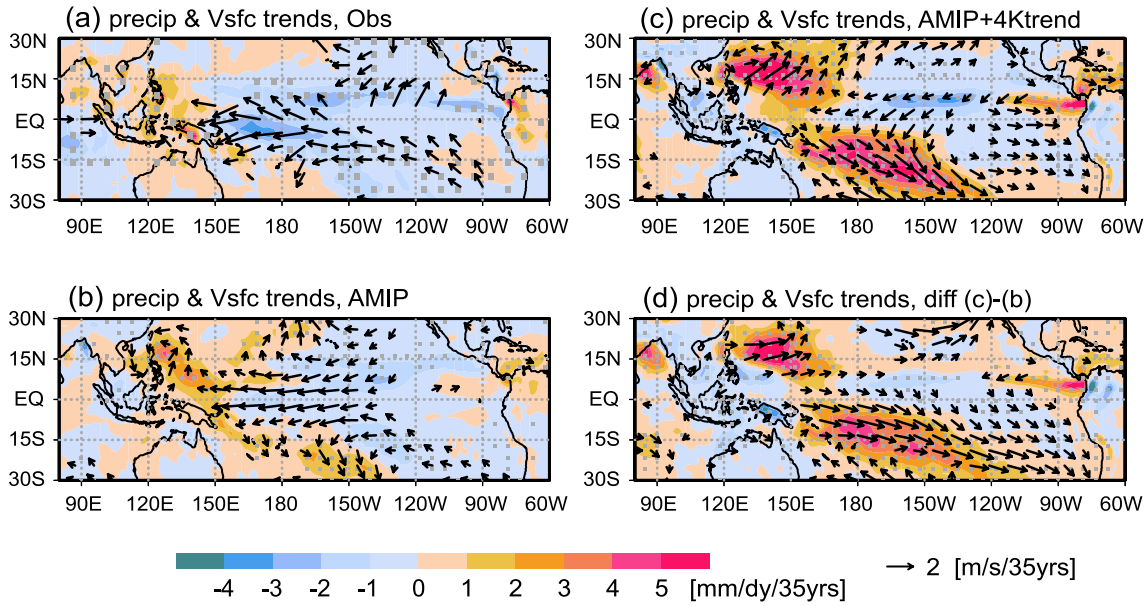

Figure 3. Trend patterns induced by the SST trend pattern and uniform warming. (a) Linear trends for 1971–2013 in precipitation (shading) and surface winds (vector) in Global Precipitation Climatology Project (GPCP) observation (Adler et al., 2018) and the JRA55, and (b) as in (a) but for the ensemble mean of the AMIP experiment. The precipitation trends statistically significant at the 95% level are stippled. The wind trends are plotted for the magnitude greater than 1 m s^{-1} in JRA55 and 0.5 m s^{-1} per 35 years in the AMIP. (c, d) As in (b) but for the trends in the AMIP+4Ktrend and their difference from the AMIP.

Associated with the PWC weakening with increasing global warming level, the net climate feedback becomes less negative (from −2.4 W m^2 K^{-1} in AMIP to −1.8 W m^2 K^{-1} in AMIP+4Ktrend; see Figure S4 in Supporting Information S1), indicating that the HS mechanism explains the state-dependence of the climate feedback distinct from the pattern effect because the SST trend pattern is identical among the experiments.

In the climatological mean state, water vapor has a broad horizontal structure compared to precipitation and mass flux in the tropics (Figure S5 in Supporting Information S1) and the increase with warming causes the mass flux to reduce (Figure 2b). However, the mass flux can increase over limited regions where precipitation increases, which should happen because both quantities measure the convective activity. In tropical atmospheric dynamics, circulation anomaly is coupled to diabatic heating due mainly to condensation, corresponding to the precipitation anomaly. Therefore, comparing precipitation trends among the AMIP-trend experiments could reveal mechanisms of the PWC strengthening and weakening by the SST pattern change and uniform warming, respectively.

Observed trends in precipitation for 1979–2013 show an increase over the western Pacific and a decrease over the central-eastern basin in association with the intensified trade winds (Figure 3a). This pattern is well reproduced in the AMIP run, which approximates the effect of the SST trend pattern as the difference from the AMIP+0K-trend is very small (Figure 3b). In the AMIP+4Ktrend, precipitation considerably increases over the subtropical Pacific, which accompanies surface westerly trends (Figure 3c). The effect of the uniform warming trend is then extracted by the difference between the AMIP and AMIP+4Ktrend, showing the pattern of precipitation trend that has a meridional, but not zonal, contrast unlike the trend in the AMIP and observations (Figure 3d). In the global warming response, enhanced radiative cooling and tropospheric stability both act to counteract the increased condensational heating (Kang et al., 2023; Knutson & Manabe, 1995; Ma et al., 2012), the features also identified in our experiments (Figures S6 and S7 in Supporting Information S1). However, those effects are relatively zonally homogeneous besides are not yet visible in the past, and therefore the PWC strengthening is reproduced solely by the precipitation pattern change using a simple linear dynamical computation (Figure S8 and Text S3 in Supporting Information S1). In summary, an increase in the zonal contrast of precipitation in the tropical Pacific is the key counterpart to the past PWC strengthening.

4. Further Attribution of the PWC Trend to Regional SST Pattern Change

To identify regions of the SST pattern change responsible for the PWC strengthening, we repeated the AMIP run but with the SST trend confined to the Northern Hemisphere (10°−90°N), the Southern Hemisphere (10°−90°S),

19448007, 2023, 23, Downloaded from https://agupubs.onlinelibrary.wiley.com/doi/10.1029/2023GL105332 by Cochrane Germany, Wiley Online Library on [12/12/2023]. See the Terms and Conditions (https://onlinelibrary.wiley.com/terms-and-conditions) on Wiley Online Library for rules of use; OA articles are governed by the applicable Creative Commons License

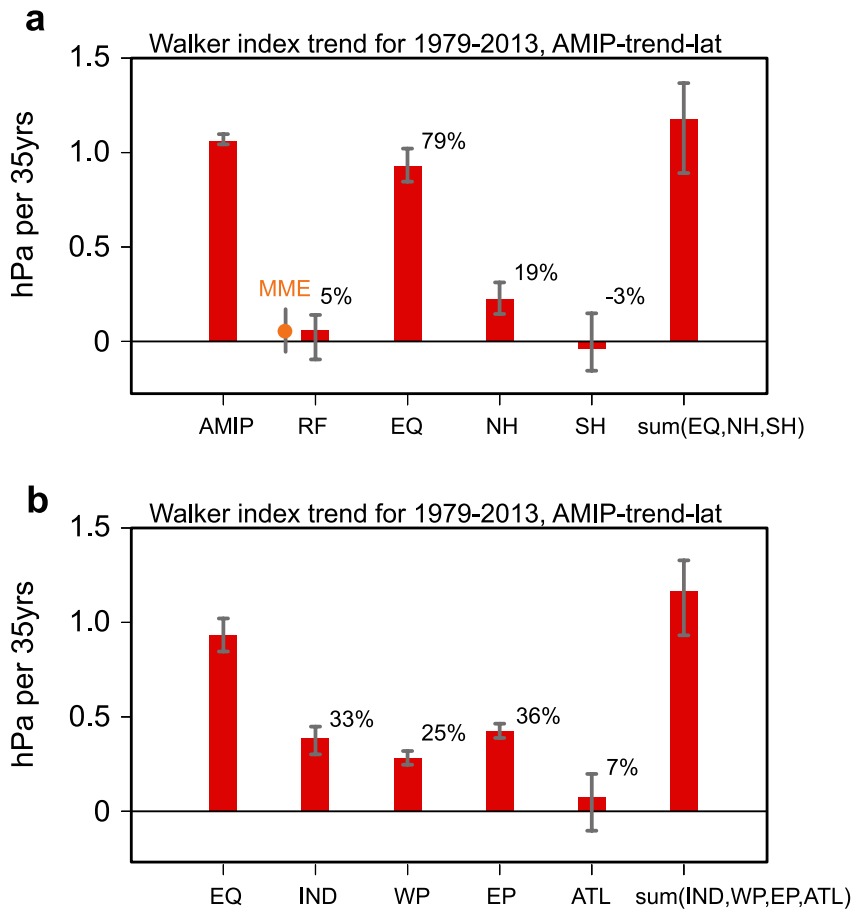

Figure 4. Attribution of the Pacific Walker circulation trend to the regional SST trend. (a) Linear trend of the Walker index in the AMIP experiment (left) and the trend due to direct radiative forcing (RF), SST trend in the equatorial band (EQ), Northern Hemisphere (NH), Sothern Hemisphere (SH), and their sum. The fractional percentage of each contribution is shown by numbers. The orange dot with the gray line indicates the trend due to RF obtained from AMIP-piForcing experiments by 8 models. (b) As in (a) but for the attribution of the Walker index trend in the AMIP-EQtrend into the trend due to the Indian Ocean (IND), western Pacific (WP), eastern Pacific (EP), and Atlantic (ATL) SST trends. See Section 4 for the description of the experiments.

and the equatorial band (10°S–10°N), called the AMIP-NHtrend, AMIP-SHtrend, and AMIP-EQtrend experiments. The equatorial SST trend is further decomposed into the Indian Ocean (40°−120°E), western Pacific (120°−170°E), eastern Pacific (170°E −70°W), and Atlantic (70°W −20°E) (Figure S9 in Supporting Information S1). Because part of the PWC trends in the AMIP experiment might come from the direct radiative forcing (Bony et al., 2013), the effect is separately estimated using the so-called AMIP-piForcing experiment (Andrews et al., 2018). The regional SST trends are in reality not independent of each other, especially in the equatorial Pacific, but the above experiments could give us a hint of the primary trigger for the PWC strengthening.

It is found that the impacts of SST trend patterns in three latitudinal bands on the PWC intensification are roughly additive and the warming pattern in the equatorial strip is the most effective contributor, accounting for 79% of the PWC trend seen in the AMIP (Figure 4a). Both the direct radiative forcing and the Southern Hemisphere SST trends have negligible impact whereas the Northern Hemisphere SST trends explain 19% of the PWC trend, due perhaps to a remote influence of the surface warming pattern associated with changing aerosols emission.

Additional attribution experiments show that the SST trends in the equatorial Indian Ocean and the Pacific are equally important but the equatorial Atlantic has a minor impact on the PWC trend (Figure 4b; Figure S10 in Supporting Information S1). It is not surprising that the PWC trend is driven by the in-situ SST trend pattern in the Pacific, but a direct impact of the Indian Ocean warming pattern, accounting for about one-third of the total impact of the equatorial SST trends, is an intriguing result. It is noted, however, the fractional contribution

19448007, 2023, 23, Downloaded from https://agupubs.onlinelibrary.wiley.com/doi/10.1029/2023GL105332 by Cochrane Germany, Wiley Online Library on [12/12/2023]. See the Terms and Conditions (https://onlinelibrary.wiley.com/terms-and-conditions) on Wiley Online Library for rules of use; OA articles are governed by the applicable Creative Commons License

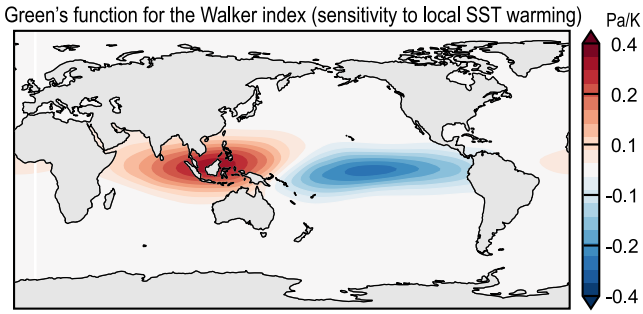

Figure 5. Green's function of the Pacific Walker circulation (PWC) to local SST warming. Response of the annual-mean Walker index to a unit of SST warming at each grid box, obtained from the CAM4 Green's function experiment. The units are Pa K^{-1}. Positive values indicate that the PWC strengthens in response to an SST increase there and vice versa for negative values.

of the Indian Ocean warming to the PWC trend depends on the definition of the Walker circulation index (Figure S11 in Supporting Information S1). The contribution remains similar (31%) when the PWC is measured by the surface zonal wind in the equatorial Pacific but reduces to 9% when the eastern Indian Ocean is excluded from the SLP-based Walker index.

The above result is further supported using the Green's function experiment, in which a patch of warm SST anomaly is given to 137 locations over the globe to identify the pattern effect on climate feedback (Dong et al., 2019). This experiment was done using a different model, NCAR's Community Atmosphere Model version 4.0, but the sensitivity map of the PWC response to local SST forcing, that is, Green's function, shows that the equatorial Indian Ocean warming, in addition to the equatorial Pacific warming and cooling, is effective in altering the PWC (Figure 5). Another support is obtained from the Indian Ocean pacemaker experiments (Mochizuki et al., 2016; Zhang et al., 2019), which show the acceleration of trade winds compared to the historical run based on the same GCM although the extent to which the observed Indian Ocean warming impacts the tropical Pacific is dependent on the model.

The attribution analysis based on our AMIP-trend experiments suggests that the tropical basin coupling and the atmosphere-ocean interaction within the equatorial Pacific are the major drivers for the past PWC intensification. However, this does not deny the possibility that the extratropical forcing, for example, Southern Ocean cooling (Kim et al., 2022), can be a factor for the PWC trend because our experiments do not represent, by definition, remote mechanisms mediated by atmosphere-ocean coupling. Yet, it is clear that, for such a remote mechanism to work, SST in the narrow equatorial strip has to change. Likewise, tropical Atlantic warming may also be a driver if it affects the eastern equatorial Pacific (McGregor et al., 2014) or the Indian Ocean SST trends (Li et al., 2016).

5. Discussion

5.1. Possible Role of Forced Change Versus Internal Variability

In this study, we have not discussed the relative role of the forced response and internal variability in the observed PWC intensification. To fully address this issue, the cause of the global SST trend pattern needs to be investigated, which is beyond our scope. Nevertheless, we could infer that the Indian Ocean warming impact on the PWC trend (Figures 4b and 5) represents the forced response.

When forced response is defined with an ensemble mean of single-model large-ensemble historical simulations following previous studies (Chung et al., 2019; Watanabe et al., 2021), the forced SST trend in the Indian Ocean, as well as the tropical Atlantic and some regions in the northern extratropics, is more than twice as large as the trend due to internal variability (Figure S12 in Supporting Information S1). This signal-to-noise pattern may be partly model-dependent but suggests that the Indian Ocean warming partly responsible for the PWC intensification is unlikely due to internal variability. In contrast, the signal-to-noise ratio is small in the equatorial Pacific, which indicates that the local impact on the PWC intensification, accounting for 60% of the trend in AMIP, represents internal variability to a large extent. A recent study suggests that the relative warming of the Indian Ocean has been explained by the radiative forcing associated with biomass burning aerosols, which are uncertain in current GCMs (Tian et al., 2023), and therefore underrepresented forced SST response may partly explain the discrepancy of the PWC trend between observations and models.

5.2. Implications for Future Projections

The majority of climate simulations forced by future emission scenarios show enhanced warming of the equatorial central-eastern Pacific compared to the other tropical basins, driving the PWC weakening (IPCC, 2021). Those changes are supported by an idealized abrupt $4 \times CO_2$ experiment by MIROC6, in which the PWC response scales well with the rise of global-mean surface temperature (Figure S13 in Supporting Information S1). During the late period of the 150 years simulation, the PWC weakening is greater than double that in the AMIP+4Ktrend,

19448007, 2023, 23, Downloaded from https://agupubs.onlinelibrary.wiley.com/doi/10.1029/2023GL105332 by Cochrane Germany, Wiley Online Library on [12/12/2023]. See the Terms and Conditions (https://onlinelibrary.wiley.com/terms-and-conditions) on Wiley Online Library for rules of use; OA articles are governed by the applicable Creative Commons License

19448007, 2023, 23, Downloaded from https://agupubs.onlinelibrary.wiley.com/doi/10.1029/2023GL105332 by Cochrane Germany, Wiley Online Library on [12/12/2023]. See the Terms and Conditions (https://onlinelibrary.wiley.com/terms-and-conditions) on Wiley Online Library for rules of use; OA articles are governed by the applicable Creative Commons License

indicating that the pattern effect acts to further slow down the PWC via the Bjerknes feedback in a similar manner to the past trend but with the opposite direction (He & Soden, 2015). The future changes in the SST pattern and thereby the PWC in the tropical Pacific are still subject to uncertainty (Han & Zheng, 2023) but, given the multi-decadal change in the past PWC trend during the instrumental era (Figure S1 in Supporting Information S1), it is likely that the SST trend pattern as observed in the recent decades will not last for a century and then the global warming influence to weaken the PWC will eventually dominate.

Conflict of Interest

The authors declare no conflicts of interest relevant to this study.

Data Availability Statement

ERSSTv5 and GPCP v2.3 data sets are available from the NOAA/OAR/ESRL PSD website (https://www.esrl.noaa.gov/psd/data/gridded/). JRA55 reanalysis data can be downloaded from the Japan Meteorological Agency website at https://jra.kishou.go.jp/JRA-55/index_en.html and ERA5 reanalysis data are available from the Copernicus Climate Service at https://cds.climate.copernicus.eu/, respectively. HadSLP2 data are open from the Met Office website at https://www.metoffice.gov.uk/hadobs/hadslp2/. The CMIP6 model outputs analyzed in this study are available from the Earth System Grid Federation (ESGF) server (https://esgf-node.llnl.gov/search/cmip6/). The Fortran codes and data used for creating the main plots in this study are available at https://ccsr.aori.u-tokyo.ac.jp/~hiro/data/amip-trend/. The archived data of the AMIP-trend experiments are available on the Zenodo repository at https://zenodo.org/record/8303209.

Acknowledgments
We thank Weiqing Han and Fei-Fei Jin for the valuable discussion on an early version of this work. M.W. and T.I. were supported by the Program for Advanced Studies of Climate Change Projection (SENTAN) Grant-in-Aid JPMXD0722680395 from the Ministry of Education, Culture, Sports, Science and Technology (MEXT), Japan. Y.D. was supported by the NOAA Climate and Global Change Postdoctoral Fellowship Program, administered by UCAR's Cooperative Programs for the Advancement of Earth System Science (CPAESS) under the award NA210AR4310383. S.M.K. was supported by the Research Program for the carbon cycle between oceans, land, and atmosphere of the National Research Foundation (NRF) funded by the Ministry of Science and ICT (NRF-2022M3I6A1090965).

References

Adler, R. F., Sapiano, M., Huffman, G., Wang, J. J., Gu, G., Bolvin, D., et al. (2018). The Global Precipitation Climatology Project (GPCP) monthly analysis (new version 2.3) and a review of 2017 global precipitation. *Atmosphere*, *9*(4), 138. https://doi.org/10.3390/atmos9040138

Andrews, T., Gregory, J. M., Paynter, D., Silvers, L. G., Zhou, C., Mauritsen, T., et al. (2018). Accounting for changing temperature patterns increases historical estimates of climate sensitivity. *Geophysical Research Letters*, *45*(16), 8490–8499. https://doi.org/10.1029/2018gl078887

Bjerknes, J. (1969). Atmospheric teleconnections from the equatorial Pacific. *Monthly Weather Review*, *97*(3), 162–172. https://doi.org/10.1175/1520-0493(1969)097<0163:atftep>2.3.co;2

Bony, S., Bellon, G., Klocke, D., Sherwood, S., Fermepin, S., & Denvil, S. (2013). Robust direct effect of carbon dioxide on tropical circulation and regional precipitation. *Nature Geoscience*, *6*, 447–451. https://doi.org/10.1038/ngeo1799

Bordbar, M. H., Martin, T., Latif, M., & Park, W. (2017). Role of internal variability in recent decadal to multidecadal tropical Pacific climate changes. *Geophysical Research Letters*, *44*(9), 4246–4255. https://doi.org/10.1002/2016gl072355

Ceppi, P., & Gregory, J. M. (2017). Relationship of tropospheric stability to climate sensitivity and Earth's observed radiation budget. *Proceedings of the National Academy of Sciences of the United States of America*, *114*(50), 13126–13131. https://doi.org/10.1073/pnas.1714308114

Chadwick, R., Boutle, I., & Martin, G. (2013). Spatial patterns of precipitation change in CMIP5: Why the rich do not get richer in the tropics. *Journal of Climate*, *26*(11), 3803–3822. https://doi.org/10.1175/jcli-d-12-00543.1

Chadwick, R., Good, P., Andrews, T., & Martin, G. (2014). Surface warming patterns drive tropical rainfall pattern responses to CO_2 forcing on all timescales. *Geophysical Research Letters*, *41*(2), 610–615. https://doi.org/10.1002/2013gl058504

Chung, E. S., Timmermann, A., Soden, B. J., Ha, K.-J., Shi, L., & John, V. O. (2019). Reconciling opposing Walker circulation trends in observations and model projections. *Nature Climate Change*, *9*(5), 405–412. https://doi.org/10.1038/s41558-019-0446-4

Coats, S., & Karnauskas, K. (2017). Are simulated and observed twentieth century tropical Pacific sea surface temperature trends significant relative to internal variability? *Geophysical Research Letters*, *44*(19), 9928–9937. https://doi.org/10.1002/2017gl074622

DeAngelis, A., Qu, X., Zelinka, M., & Hall, A. (2015). An observational radiative constraint on hydrologic cycle intensification. *Nature*, *528*(7581), 249–253. https://doi.org/10.1038/nature15770

Dong, Y., Pauling, A. G., Sadai, S., & Armour, K. C. (2022). Antarctic ice-sheet meltwater reduces transient warming and climate sensitivity through the sea-surface temperature pattern effect. *Geophysical Research Letters*, *49*(24), e2022GL101249. https://doi.org/10.1029/2022gl101249

Dong, Y., Proistosescu, C., Armour, K. C., & Battisti, D. S. (2019). Attributing historical and future evolution of radiative feedbacks to regional warming patterns using a Green's function approach: The preeminence of the western Pacific. *Journal of Climate*, *32*(17), 5471–5491. https://doi.org/10.1175/jcli-d-18-0843.1

England, M., McGregor, S., Spence, P., Meehl, G. A., Timmermann, A., Cai, W., et al. (2014). Recent intensification of wind-driven circulation in the Pacific and the ongoing warming hiatus. *Nature Climate Change*, *4*(3), 222–227. https://doi.org/10.1038/nclimate2106

England, M. R., Polvani, L. M., Sun, L., & Deser, C. (2020). Tropical climate responses to projected Arctic and Antarctic sea-ice loss. *Nature Geoscience*, *13*(4), 275–281. https://doi.org/10.1038/s41561-020-0546-9

Eyring, V., Bony, S., Meehl, G. A., Senior, C. A., Stevens, B., Stouffer, R. J., & Taylor, K. E. (2016). Overview of the Coupled Model Intercomparison Project Phase 6 (CMIP6) experimental design and organization. *Geoscientific Model Development*, *9*(5), 1937–1958. https://doi.org/10.5194/gmd-9-1937-2016

Fläschner, D., Mauritsen, T., & Stevens, B. (2016). Understanding the intermodel spread in global-mean hydrological sensitivity. *Journal of Climate*, *29*(2), 801–817. https://doi.org/10.1175/jcli-d-15-0351.1

Gates, W. L., Boyle, J. S., Covey, C., Dease, C. G., Doutriaux, C. M., Drach, R. S., et al. (1999). An overview of the results of the atmospheric model Intercomparison Project (AMIP I). *Bulletin America Meteorology Social*, *73*(12), 1962–1970. https://doi.org/10.1175/1520-0477(1992)073<1962:atamip>2.0.co;2

Han, Z. W., & Zheng, X. T. (2023). Intermodel uncertainty in response of the Pacific Walker circulation to global warming. *Climate Dynamics*, *61*(5–6), 2317–2337. in press. https://doi.org/10.1007/s00382-023-06685-y

He, J., & Soden, B. J. (2015). Anthropogenic weakening of the tropical circulation: The relative roles of direct CO_2 forcing and sea surface temperature change. *Journal of Climate*, *28*(22), 8728–8742. https://doi.org/10.1175/jcli-d-15-0205.1

Heede, U., & Fedorov, A. (2021). Eastern equatorial Pacific warming delayed by aerosols and thermostat response to CO_2 increase. *Nature Climate Change*, *11*(8), 696–704. https://doi.org/10.1038/s41558-021-01101-x

Heede, U. K., Fedorov, A. V., & Burls, N. J. (2020). Time scales and mechanisms for the tropical Pacific response to global warming: A tug of war between the ocean thermostat and weaker Walker. *Journal of Climate*, *33*(14), 6101–6118. https://doi.org/10.1175/jcli-d-19-0690.1

Held, I. M., & Soden, B. J. (2006). Robust responses of the hydrological cycle to global warming. *Journal of Climate*, *19*(21), 5686–5699. https://doi.org/10.1175/jcli3990.1

Henley, B. J., Meehl, G., Power, S. B., Folland, C. K., King, A. D., Brown, J. N., et al. (2017). Spatial and temporal agreement in climate model simulations of the Interdecadal Pacific Oscillation. *Environmental Research Letters*, *12*(4), 044011. https://doi.org/10.1088/1748-9326/aa5cc8

Huang, B., Thorne, P. W., Banzon, V. F., Boyer, T., Chepurin, G., Lawrimore, J. H., et al. (2017). Extended reconstructed sea surface temperature, version 5 (ERSSTv5): Upgrades, validations, and intercomparisons. *Journal of Climate*, *30*(20), 8179–8205. https://doi.org/10.1175/jcli-d-16-0836.1

Huang, P., Xie, S.-P., Hu, K., Huang, G., & Huang, R. (2013). Patterns of the seasonal response of tropical rainfall to global warming. *Nature Geoscience*, *6*(5), 357–361. https://doi.org/10.1038/ngeo1792

IPCC. (2021). Climate change 2021: The physical science basis. In *Contribution of working group I to the sixth assessment report of the intergovernmental panel on climate change*. Cambridge University Press. https://doi.org/10.1017/9781009157896

Jin, F.-F. (1996). Tropical ocean-atmosphere interaction, the Pacific cold tongue, and the El Niño Southern Oscillation. *Science*, *274*(5284), 76–78. https://doi.org/10.1126/science.274.5284.76

Kang, S. M., Shin, Y., Kim, H., Xie, S.-P., & Hu, S. (2023). Disentangling the mechanisms of equatorial Pacific climate change. *Science Advances*, *9*(19), eadf5059. https://doi.org/10.1126/sciadv.adf5059

Kim, H., Kang, S. M., Kay, J. E., & Xie, S.-P. (2022). Subtropical clouds key to Southern Ocean teleconnections to the tropical Pacific. *Proceedings of the National Academy of Sciences of the United States of America*, *119*(34), e2200514119. https://doi.org/10.1073/pnas.2200514119

Knutson, T. R., & Manabe, S. (1995). Time-mean response over the tropical Pacific to increased CO_2 in a coupled ocean-atmosphere model. *Journal of Climate*, *8*(9), 2181–2199. https://doi.org/10.1175/1520-0442(1995)008<2181:tmrott>2.0.co;2

Kobayashi, S., Ota, Y., Harada, Y., Ebita, A., Moriya, M., Onoda, H., et al. (2015). The JRA-55 reanalysis: General specifications and basic characteristics. *Journal of the Meteorological Society of Japan*, *93*(1), 5–48. https://doi.org/10.2151/jmsj.2015-001

Lee, S., L'Heureux, M., Wittenberg, A. T., Seager, R., O'Gorman, P. A., & Johnson, N. C. (2022). On the future zonal contrasts of equatorial Pacific climate: Perspectives from observations, simulations, and theories. *Npj Climate and Atmospheric Science*, *5*(1), 82. https://doi.org/10.1038/s41612-022-00301-2

Li, X., Xie, S.-P., Gille, S. T., & Yoo, C. (2016). Atlantic-induced pan-tropical climate change over the past three decades. *Nature Climate Change*, *6*(3), 275–279. https://doi.org/10.1038/nclimate2840

Loeb, N. G., Wang, H., Allan, R. P., Andrews, T., Armour, K., Cole, J. N. S., et al. (2020). New generation of climate models track recent unprecedented changes in Earth's radiation budget observed by CERES. *Geophysical Research Letters*, *47*(5), e2019GL086705. https://doi.org/10.1029/2019gl086705

Ma, J., Xie, S.-P., & Kosaka, Y. (2012). Mechanisms for tropical tropospheric circulation change in response to global warming. *Journal of Climate*, *25*(8), 2979–2994. https://doi.org/10.1175/jcli-d-11-00048.1

McGregor, S., Timmermann, A., Stuecker, M., England, M. H., Merrifield, M., Jin, F.-F., & Chikamoto, Y. (2014). Recent Walker circulation strengthening and Pacific cooling amplified by Atlantic warming. *Nature Climate Change*, *4*(10), 888–892. https://doi.org/10.1038/nclimate2330

Merlis, T. M., & Schneider, T. (2011). Changes in zonal surface temperature gradients and Walker circulations in a wide range of climates. *Journal of Climate*, *24*(17), 4757–4768. https://doi.org/10.1175/2011jcli4042.1

Mochizuki, T., Kimoto, M., Watanabe, M., Chikamoto, Y., & Ishii, M. (2016). Interbasin effects of the Indian Ocean on Pacific decadal climate change. *Geophysical Research Letters*, *43*(13), 7168–7175. https://doi.org/10.1002/2016gl069940

O'Reilly, C. H., Patterson, M., Robson, J., Monerie, P. A., Hodson, D., & Ruprich-Robert, Y. (2023). Challenges with interpreting the impact of Atlantic multidecadal variability using SST-restoring experiments. *Npj Climate and Atmospheric Science*, *6*(1), 14. https://doi.org/10.1038/s41612-023-00335-0

Power, S., Casey, T., Folland, C., Colman, A., & Mehta, V. (1999). Inter-decadal modulation of the impact of ENSO on Australia. *Climate Dynamics*, *15*(5), 319–324. https://doi.org/10.1007/s003820050284

Sandeep, S., Stordal, F., Sardeshmukh, P. D., & Compo, G. P. (2014). Pacific Walker circulation variability in coupled and uncoupled climate models. *Climate Dynamics*, *43*(1–2), 103–117. https://doi.org/10.1007/s00382-014-2135-3

Seager, R., Cane, M., Henderson, N., Lee, D.-E., Abernathey, R., & Zhang, H. (2019). Strengthening tropical Pacific zonal sea surface temperature gradient consistent with rising greenhouse gases. *Nature Climate Change*, *9*(7), 517–522. https://doi.org/10.1038/s41558-019-0505-x

Seager, R., Henderson, N., & Cane, M. (2022). Persistent discrepancies between observed and modeled trends in the tropical Pacific Ocean. *Journal of Climate*, *35*(14), 4571–4584. https://doi.org/10.1175/jcli-d-21-0648.1

Shrestha, S., & Soden, B. J. (2023). Anthropogenic weakening of the atmospheric circulation during the satellite era. *Geophysical Research Letters*, *50*, e2023GL104784. https://doi.org/10.1029/2023GL104784

Smith, D., Booth, B. B. B., Dunstone, N. J., Eade, R., Hermanson, L., Jones, G. S., et al. (2016). Role of volcanic and anthropogenic aerosols in the recent global surface warming slowdown. *Nature Climate Change*, *6*(10), 936–940. https://doi.org/10.1038/nclimate3058

Stevens, B., Sherwood, S. C., Bony, S., & Webb, M. J. (2016). Prospects for narrowing bounds on Earth's equilibrium climate sensitivity. *Earth's Future*, *4*(11), 512–522. https://doi.org/10.1002/2016ef000376

Takahashi, C., & Watanabe, M. (2016). Pacific trade winds accelerated by aerosol forcing over the past two decades. *Nature Climate Change*, *6*(8), 768–772. https://doi.org/10.1038/nclimate2996

Tatebe, H., Ogura, T., Nitta, T., Komuro, Y., Ogochi, K., Takemura, T., et al. (2019). Description and basic evaluation of simulated mean state, internal variability, and climate sensitivity in MIROC6. *Geoscientific Model Development*, *12*(7), 2727–2765. https://doi.org/10.5194/gmd-12-2727-2019

Tian, Y., Hu, S., & Deser, C. (2023). Critical role of biomass burning aerosols in enhanced historical Indian Ocean warming. *Nature Communications*, *14*(1), 3508. https://doi.org/10.1038/s41467-023-39204-y

Tokinaga, H., Xie, S.-P., Deser, C., Kosaka, Y., & Okumura, Y. (2012). Slowdown of the Walker circulation driven by tropical Indo-Pacific warming. *Nature*, *491*(7424), 439–443. https://doi.org/10.1038/nature11576

19448007, 2023, 23, Downloaded from https://agupubs.onlinelibrary.wiley.com/doi/10.1029/2023GL105332 by Cochrane Germany, Wiley Online Library on [12/12/2023]. See the Terms and Conditions (https://onlinelibrary.wiley.com/terms-and-conditions) on Wiley Online Library for rules of use; OA articles are governed by the applicable Creative Commons License

Vecchi, G., Soden, B. J., Wittenberg, A. T., Held, I. M., Leetmaa, A., & Harrison, M. J. (2006). Weakening of tropical Pacific atmospheric circulation due to anthropogenic forcing. *Nature*, *441*(7089), 73–76. https://doi.org/10.1038/nature04744

Vecchi, G. A., & Soden, B. J. (2007). Global warming and the weakening of the tropical circulation. *Journal of Climate*, *20*(17), 4316–4434. https://doi.org/10.1175/jcli4258.1

Watanabe, M., Dufresne, J.-L., Kosaka, Y., Mauritsen, T., & Tatebe, H. (2021). Enhanced warming constrained by past trends in equatorial Pacific sea surface temperature gradient. *Nature Climate Change*, *11*(1), 33–37. https://doi.org/10.1038/s41558-020-00933-3

Wills, R., Dong, Y., Proistosecu, C., Armour, K., & Battisti, D. (2022). Systematic climate model biases in the large-scale patterns of recent sea-surface temperature and sea-level pressure change. *Geophysical Research Letters*, *49*(17), e2022GL100011. https://doi.org/10.1029/2022gl100011

Wu, M., Zhou, T., Li, C., Li, H., Chen, X., Wu, B., et al. (2021). A very likely weakening of Pacific Walker Circulation in constrained near-future projections. *Nature Communications*, *12*(1), 6502. https://doi.org/10.1038/s41467-021-26693-y

Xie, S.-P. (2022). *Coupled atmosphere-ocean dynamics* (p. 432). Elsevier.

Xie, S.-P., Deser, C., Vecchi, G., Ma, J., Teng, H., & Wittenberg, A. (2010). Global warming pattern formation: Sea surface temperature and rainfall. *Journal of Climate*, *23*(4), 966–986. https://doi.org/10.1175/2009jcli3329.1

Zhang, L., Han, W., Karnauskas, K. B., Meehl, G. A., Hu, A., Rosenbloom, N., & Shinoda, T. (2019). Indian Ocean warming trend reduces Pacific warming response to anthropogenic greenhouse gases: An interbasin thermostat mechanism. *Geophysical Research Letters*, *46*(19), 10882–10890. https://doi.org/10.1029/2019gl084088

Zhou, C., Zelinka, M., & Klein, S. (2016). Impact of decadal cloud variations on the Earth's energy budget. *Nature Geoscience*, *9*(12), 871–874. https://doi.org/10.1038/ngeo2828

Zhou, Z., Xie, S.-P., Zhang, G. J., & Zhou, W. (2018). Evaluating AMIP skill in simulating interannual variability over the Indo–western Pacific. *Journal of Climate*, *31*(6), 2253–2265. https://doi.org/10.1175/jcli-d-17-0123.1

19448007, 2023, 23, Downloaded from https://agupubs.onlinelibrary.wiley.com/doi/10.1029/2023GL105332 by Cochrane Germany, Wiley Online Library on [12/12/2023]. See the Terms and Conditions (https://onlinelibrary.wiley.com/terms-and-conditions) on Wiley Online Library for rules of use; OA articles are governed by the applicable Creative Commons License